Macromolecules

ARTICLE

pubs.acs.org/Macromolecules

Decompression-Induced Encapsulation of Core-philic Solutes by Block Copolymer Micelles in Compressible Solutions: Polystyrene and Polystyrene-*block*-polybutadiene in Near-Critical Propane

Winoto Winoto and Maciej Radosz*

Soft Materials Laboratory, Department of Chemical & Petroleum Engineering, University of Wyoming, Laramie, Wyoming 82071-3295, United States

Supporting Information

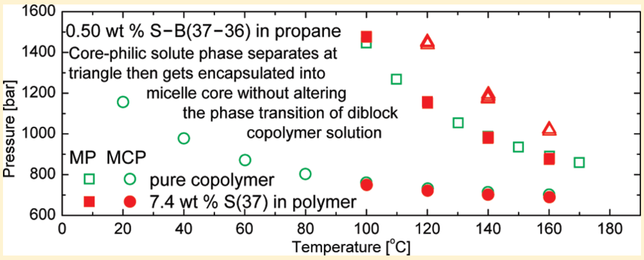

ABSTRACT: Pressure-tuned propane capacity and selectivity for polystyrene-*block*-polybutadiene allows for random molecular solutions at high pressures, micellar solutions at moderate pressures, and bulk phase separation at low pressures. While corona-philic homopolymer solutes primarily stay in solution when the micelles are formed, core-philic homopolymer solutes, such as polystyrene, are found to concentrate in and hence become encapsulated by the micelle core. If the concentration of such a block-sized polystyrene solute is in the right range, say up to 15 wt % on a solvent-free basis, it can produce an encapsulation peak on either the transmitted-light intensity trace or the scattered-light intensity trace, or both. Such encapsulation peaks can help detect the onset of micellization and encapsulation, especially when guided by a macromolecular model, such as statistical associating fluid theory (SAFT1), used to estimate the onset of bulk phase transitions in this work. A core-philic solute, free polystyrene in this case, does not alter the crucial micellization pressure or even the micellar cloud pressure, at which the micelles coalesce and precipitate from solution in bulk.

INTRODUCTION

Block copolymers can self-assemble in solutions and melts to form well-known nanosized structures which usually depend on the block ratio. When, in addition to copolymer itself and solvent, other minor solutes are present, they partition between the bulk phase and nanophase according to their affinities, quantified for example with their chemical potentials. Such minor components can be intentional, for example, hydrophobic drugs that are to be encapsulated by micelle cores toward drug-delivery nanoparticles or tolerated but unintentional, for example, free unreacted homopolymers or other impurities. Among the few clues on how unintentional solutes may affect block copolymer structures, the copolymer order−disorder transition was found[1] to change slightly due to homopolymer presence, but the change was not noticeable below several percent of homopolymer. In another example, undesirable homopolymer impurities were found to cause a scattering peak[2] upon micellization of copolymer in dilute solution, previously referred to as "anomalous micellization". However, such homopolymer impurities were not found[3] to shift the micellization conditions.

For micelles formed in dilute solutions, one can divide other minor solutes into those that have affinity for the micelle corona, and hence are referred to as corona-philic solutes, and those that have affinity for the micelle core, and hence are referred to as core-philic solutes. The corona-philic solutes naturally prefer the solvent and hence accumulate in the solvent-rich phase; their partitioning coefficients are low. By contrast, the core-philic solutes are more likely to precipitate from solution, for the same reason that the core-forming blocks aggregate when micelles are formed, and hence their partitioning coefficients are high; their mole fractions in the core are higher, and usually much higher, than those in the solvent-rich phase. This is the basis of deliberate efforts to encapsulate core-philic solutes in micelle cores, such as cancer drugs in micellar polymeric nanoparticles.

While there is plenty of qualitative evidence pointing to the effectiveness and importance of such core-philic drug encapsulation, there is very little, if any, quantitative understanding of how such solutes interact with and impact micelle formation. Even less is known about such micellization-driven encapsulating processes in compressible solutions, for example, in sub- or supercritical fluid solvents, referred here as near-critical solvents. A unique advantage of such compressible solvents is that their capacity and selectivity can be controlled with pressure alone. For example, they have high capacity and hence low selectivity at high pressures, which leads to random molecular solutions, a higher selectivity at moderate pressures, which leads to micelle formation, and a low capacity at low pressures, which leads to micelle aggregation and bulk separation.

Received: March 17, 2011
Revised: May 14, 2011
Published: June 07, 2011

Table 1. Polymers Used in This Work

polymer	short name	M_n[a]	PDI[b]	ref[c]
polystyrene	S(5)[d]	5.5	1.02	ref 14; this work for ternary
	S(37)	36.8	1.02	ref 6
	S(87)[d]	87	1.05	ref 14
polybutadiene	B(5)[d]	5.3	1.04	ref 9; this work for ternary
	B(38)	38.2	1.05	ref 6; this work for ternary
polystyrene-*block*-polybutadiene	S–B(5–5)[d]	5.4–5.35	1.03	ref 9
	S–B(37–36)	36.8–35.9	1.01	ref 6; this work for ternary

[a] M_n = number-average molecular weight (kg/mol). [b] Polydispersity index = M_w/M_n; M_w = weight-average molecular weight. [c] Original source of tabulated data. [d] Purchased from Polymer Source, Inc. Otherwise, synthesized at Oak Ridge National Laboratory.

This theme has been the subject of our recent work on characterization of micellar and bulk phase transitions of model styrene–diene block copolymers in a compressible alkane solvent, such as propane.[4] At a constant polymer concentration, both micellization temperature and pressure were found to fall around a decreasing micellar phase boundary curve in pressure–temperature coordinates, which lies above the copolymer cloud-point curve and below the polystyrene cloud-point curve. That work also provided quantitative data on the effects of copolymer molecular weight,[5,6] block ratio,[6] crystallizability,[7] deuteration,[8] solvent,[6,7] and cloud pressure reduction[4−6,8] in micellar solutions relative to a hypothetical random solution estimated from statistical associating fluid theory.[9] However, we do not understand how the presence of a deliberately added core-philic solute can affect the micellization of a model styrene–diene block copolymer in a compressible alkane solvent, such as propane.

The goal of this work, therefore, is to characterize dilute solutions of polystyrene-*block*-polybutadiene (0.5 wt %) in propane that contain gradually increasing concentration of free polystyrene, say from 0 to about 15 wt % on a solvent-free basis. As a reference, corresponding solutions of polystyrene alone will be characterized as well. Examples of questions that we want to address are as follows: How will the transmitted- and scattered-light intensity traces respond to polystyrene addition? How can it affect the micellization pressure, if any? How can its encapsulation be detected? However, we shall not attempt to quantify precise concentration limits or polystyrene distribution between phases in this work.

■ EXPERIMENTAL SECTION

Materials. The homopolymers and diblock copolymers are the same or similar to those used in our previous work. They were synthesized via living anionic polymerization using well-established vacuum line techniques.[10,11] Briefly, the diblocks were prepared by sequential monomer addition, with sampling of the first block (polystyrene). Microstructure of the polybutadiene and polyisoprene was controlled through the choice of solvent and use of polar additions (tertiary amines and ethers).[12,13]

The polybutadiene samples are at least 90% of the 1,4-addition type for both homopolymer and diblock copolymer. The molecular weights and polydispersity indices of all samples are provided in Table 1, including their short names used throughout this paper.

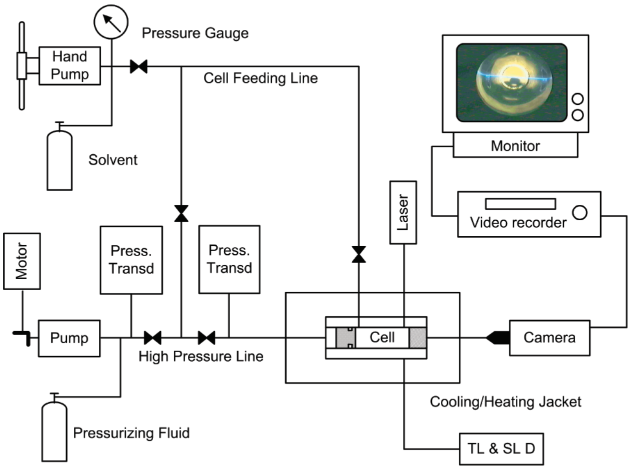

Figure 1. A simplified schematic of the apparatus.

The propane is 99.0% grade from Matheson Trigas, Inc., and used without further purification.

Experimental Method. The onset of bulk phase transition of a clear polymer solution is usually observed as the onset of turbidity, referred to as the "cloud point", that is, the pressure and temperature at which the homogeneous solution turns cloudy, characterized as the cloud pressure (CP) and the cloud temperature (CT). When the bulk phase transition occurs from a micellar solution, as opposed to a random molecular solution, such a transition is referred to as the micellar cloud point characterized by the micellar cloud pressure (MCP) and the micellar cloud temperature (MCT).

The micelle formation in a block copolymer solution is determined from the intercept at which the scattered-light intensity starts increasing upon decompression at constant temperature, which results in the micellization pressure (MP), or changing temperature at constant pressure, which results in the micellization temperature (MT). The micellization transition is reversible and occurs at the same MP and MT as the corresponding micelle decomposition transition. The micelle-containing solution is referred to as the micellar solution, in contrast to the molecular solution observed upon micelle decomposition.

In this work, CP, MCP, and MP are measured in a small high-pressure variable-volume cell, made of titanium, coupled with transmitted- and scattered-light intensity probes and equipped with a borescope for visual observation of the phase transitions and with pressure and temperature probes accurate to within ±2 bar and ±0.1 °C, respectively.

In a typical experiment, a known amount of polymer (0.5 wt %) and solvent is loaded into the cell, which is then brought to and maintained at a desired pressure and temperature, high enough for the polymer to form a homogeneous molecular solution. For a ternary solution of copolymer/homopolymer in propane, the diblock copolymer concentration is fixed at 0.5 wt %; the homopolymer content is added to this 0.5 wt % copolymer solution. A simplified schematic of the experimental setup is shown in Figure 1. A detailed description of the apparatus and experimental procedure can be found in Winoto et al.[4] In this work, attempts to reproduce CP, MCP, and MP for different cell loads suggest that the measured data are reproducible to within 30 bar.

SAFT Method for Estimating Cloud Pressures. A version of statistical associating fluid theory, referred to as SAFT1,[15] was demonstrated to represent the cloud points of molecular solutions of homopolymers and diblock copolymers in propane.[9] SAFT1 parameters used in this work are the same as those previously derived from experimental CP data for propane solutions of polystyrene,[14] polydienes, and their

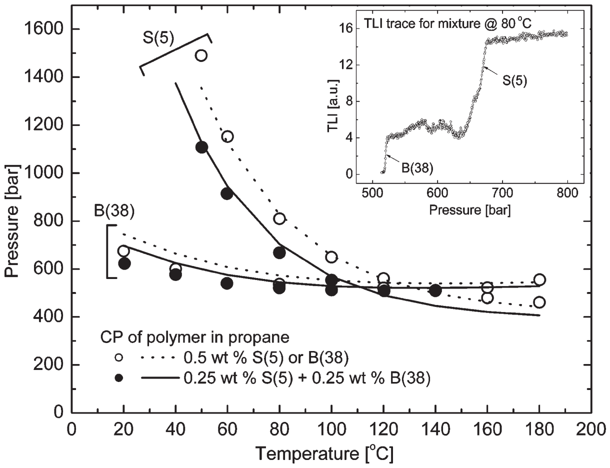

Figure 2. Cloud pressure as a function of temperature for 0.5 wt % polystyrene in propane (S(5), open points, steeper dotted curve), 0.5 wt % polybutadiene in propane (B(38), open points, flatter dotted curve), and a ternary 0.25 wt % S(5) + 0.25 wt % B(38) solution in propane (filled points, solid curves). All curves are calculated with SAFT1.

diblock copolymers.[9] Using these parameters, SAFT1 can realistically estimate CP for homopolymers and diblock copolymers in the absence of micelles, and hence in the absence of the micelle-induced cloud-pressure reduction,[5] which is a useful frame of reference. For the record, all SAFT results referred to as "curves" in the figures are for simplicity drawn as segmented lines usually calculated at the same conditions as the corresponding experimental points, but these segmented lines closely represent smooth curves.

■ RESULTS AND DISCUSSION

Free-Homopolymer versus Diblock Cloud Pressures. When two homopolymers, such as polybutadiene and polystyrene, are simultaneously dissolved in a common compressible solvent, such as propane, to form a dilute solution, they are expected to precipitate from the solution at cloud pressures that are not too different from their corresponding characteristic cloud pressures, obtained in the absence of the other polymer. This is because the interactions of the low-concentration components with each other do not affect their phase behavior substantially; in fact, they behave as if the other low-concentration components did not exist. This is illustrated in Figure 2, which shows the onset of homopolymer precipitation from solution at CP, as a function of temperature at a constant composition, for three polymer solutions in propane: two binary 0.5 wt % solutions shown with open circles (experimental data) and dotted curves (calculated SAFT1 data), the steep curve for S(5) and the flatter curve for B(38), and a ternary solution of the same polymers, 0.25 wt % S(5) + 0.25 wt % B(38), shown with filled circles (experimental data) and solid curves (calculated SAFT1 data); the ternary solution experiment is aimed at the same total polymer concentration rather than the same concentration of each polymeric component. The two CP curves observed for the ternary solution reflect two distinct CP's at each temperature, for example, below 100 °C: one that corresponds to polystyrene precipitation at higher pressure and one that corresponds to butadiene precipitation at lower pressure. This corresponds to two abrupt TLI reductions shown in the inset: one upon the polystyrene precipitation and one upon the polybutadiene reduction. Such distinct cloud pressures can be and in fact have been utilized to separate, fractionate, or purify polymer mixtures with near-critical fluids.

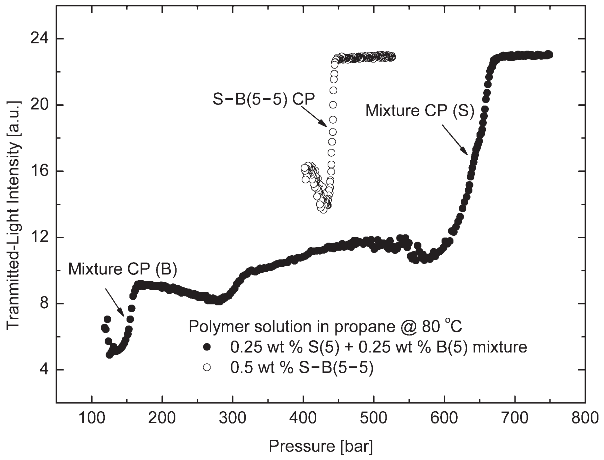

Figure 3. Transmitted-light intensity trace for cloud pressure of polystyrene (S) and polybutadiene (B) mixture (filled) and polystyrene-*block*-polybutadiene (S–B) (open).

The CP curves shown in Figure 2 exhibit a crossover around 110 °C because the two polymers are asymmetric with respect to the molecular weight (the polybutadiene molecular weight becomes dominant at higher temperatures), but this is not crucial to the point. The important point is that low-concentration homopolymers do not significantly affect each other's behavior. Another observation is that, as expected, decreasing the homopolymer concentration, say from 0.5 to 0.25 wt % in this case, produces a small but consistent reduction of cloud pressure and that all these effects are quantitatively captured by SAFT1, which can therefore be used with confidence to estimate such reference cloud pressures.

An example of a symmetric homopolymer pair, S(5) and B(5), that forms a ternary solution in propane and a matching diblock copolymer S–B(5–5) that forms a binary solution in propane, as initially reported,[9] is plotted in Figure 3 to illustrate typical TLI traces. Figure 3 shows two TLI decreases for the ternary mixture (solid points)—one around 650 bar for 0.25 wt % S(5) and one around 150 bar for 0.25 wt % B(5)—and, separately, a single decrease around 450 bar for the binary copolymer mixture (open circles). Figure 4 shows the corresponding CP curves for the binary and ternary homopolymer solutions and for the binary copolymer solution. The CP for the copolymer (open circles, dashed dotted curve) is approximately an average of the two corresponding 0.5 wt % homopolymer solution curves (dotted curves; SAFT1 calculation). As shown in both Figure 2 and 4, increasing homopolymer concentration from 0.25 to 0.5 wt % produces a more significant shift to higher cloud pressures for polystyrene than it does for polybutadiene.

Figure 4 also suggests that, since the polybutadiene CP curve is at much lower pressures than that for the copolymer, adding free polybutadiene (the corona-philic homopolymer block) should not affect the copolymer solution behavior much since the free polybutadiene will always remain in solution above the copolymer CP (as long as the butadiene block is not too much larger than the styrene block), not to mention that the free butadiene concentration is too low in this case to affect the other solutes. However, in a dilute solution that contains both free polystyrene (the core-philic homopolymer block, also referred to as S for

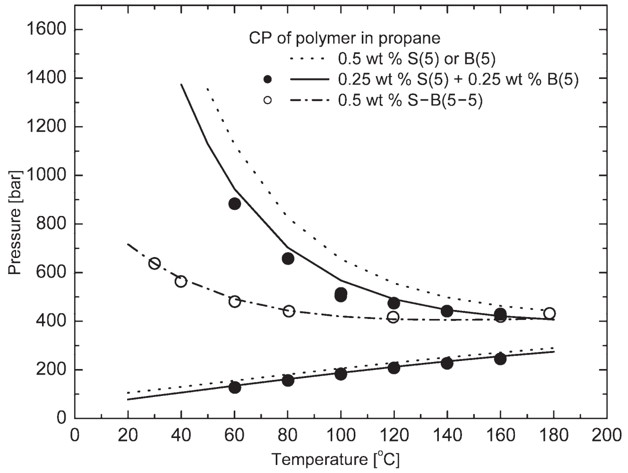

Figure 4. Cloud pressure as a function of temperature for 0.5 wt % polystyrene in propane (S(5), steeper dotted curve), 0.5 wt % polybutadiene in propane (B(38), flatter dotted curve), a ternary 0.25 wt % S(5) + 0.25 wt % B(5) solution in propane (filled points, solid curves), and 0.5 wt % polystyrene-*block*-polybutadiene in propane (S−B(5−5), open points, dashed dotted curve). The curves are estimated by SAFT1.

short) and copolymer, polystyrene can and indeed will precipitate at or around the copolymer MP. If the copolymer forms micelles, then the question is how polystyrene will affect the micellization, if any. We hypothesize that at least a fraction of polystyrene can be encapsulated by the micelle core. We shall examine this hypothesis by gradually adding polystyrene to a solution of diblock copolymer in propane, but first we need to establish a micellization and separation baseline for a propane solution of polystyrene-*block*-polybutadiene alone, with no free homopolymer present.

Polystyrene-*block*-polybutadiene Micellization and Precipitation. As mentioned before, the polystyrene-*block*-polybutadiene starts precipitating at CP that falls between the CP's of the corresponding polystyrene and polybutadiene homopolymers. When such homopolymer CP's are sufficiently different, and hence their affinities to the solvent are sufficiently different, it is a clue that the solvent selectivity with respect to each block may be sufficiently high for micelles to be formed. Conversely, a small CP difference and hence low solvent selectivity favors a random molecular solution. The micelle formation in a neat copolymer solution (free of homopolymer contamination) is typically measured as the onset of increasing SLI upon decompression. This is illustrated in Figure 5 for a 0.5 wt % S−B(37−36) solution in propane at 140 °C, where SLI starts increasing smoothly at 988 bar with no apparent peaks due to free unreacted polystyrene. In such a case, micellization pressure (MP) is declared at the intercept of the increasing SLI branch with its baseline.

This figure also illustrates a TLI trace upon decompression for the same S−B(37−36) solution in propane. Initially, at high pressures, TLI stays constant around 990 arbitrary unit (au), down to pressures slightly below MP. Upon further decompression, however, as the micelle concentration and hence SLI increases, TLI gradually decreases, say down to 800 au at 750 bar, and then it drops sharply at the onset of copolymer precipitation from micellar solution at 715 bar, which is usually taken as the micellar cloud pressure (MCP). The SLI also drops at around MCP, which means that, in this case, both TLI and SLI can be used for detecting the onset of bulk phase transition. Now the question is how this pattern will change if one adds a small, known amount of free polystyrene to such a copolymer solution, which will result in ternary solution.

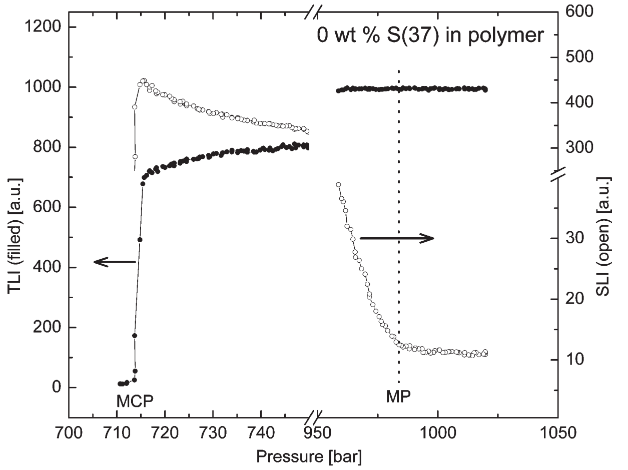

Figure 5. Transmitted- and scattered-light intensity trace for micellization pressure and micellar cloud pressure of 0.50 wt % polystyrene-*block*-polybutadiene, S−B(37−36), solution in propane at 140 °C.

Ternary Solutions: Polystyrene-*block*-polybutadiene and Block-Sized Polystyrene in Propane. In order to investigate the effect of adding free polystyrene, a ternary solution is prepared by adding polystyrene on top of the 0.5 wt % S−B(37−36) solution in propane. These additions are chosen to be 2.3, 7.4, and 14.8 wt % of S(37) that exactly matches the polystyrene block in molecular weight. Later, we shall also explore additions of 0.4 and 1.6 wt % of S(87), which exceeds the copolymer size. All these concentrations are on a solvent-free basis, but to be consistent with the context, they are occasionally converted to an overall solution basis as well. These solutions are characterized with MP and MCP curves and SLI and TLI traces.

The first example of TLI and SLI traces for a 2.3 wt % S(37)-containing S−B(37−36) solution in propane is shown in Figure 6a. The SLI starts increasing upon micellization, similar to the trace in Figure 5, which suggests that 2.3 wt % polystyrene is not enough to produce a polystyrene-induced "scattering peak". At the same time, TLI decreases slightly and, again, drops sharply at the micellar cloud pressure around 700 bar, upon the onset of bulk phase transition. These SLI and TLI traces are similar to those for plain S−B(37−36) solution shown in Figure 5. Therefore, we declare MP at the onset of SLI increase (intercept with the baseline), assuming that 2.3 wt % polystyrene is not enough to cause its precipitation peak or to affect micellization significantly. There is no experimental basis for quantifying the partitioning of polystyrene between the solution and the micelle cores, but our experience on the basis of SAFT simulations of similar systems suggests that most, if not almost all, polystyrene should be encapsulated (captured by the micelle core).

Figure 6b illustrates that the measured MP (filled squares) and MCP (filled circles) for the 2.3 wt % S(37)-containing S−B-(37−36) solution in propane are the same as those of the plain S−B(37−36) solution in propane within experimental reproducibility. For reference, Figure 6b also shows SAFT1-estimated CP (solid curve) and experimentally determined CP (open triangles) for 0.5 wt % polystyrene S(37) in propane, which

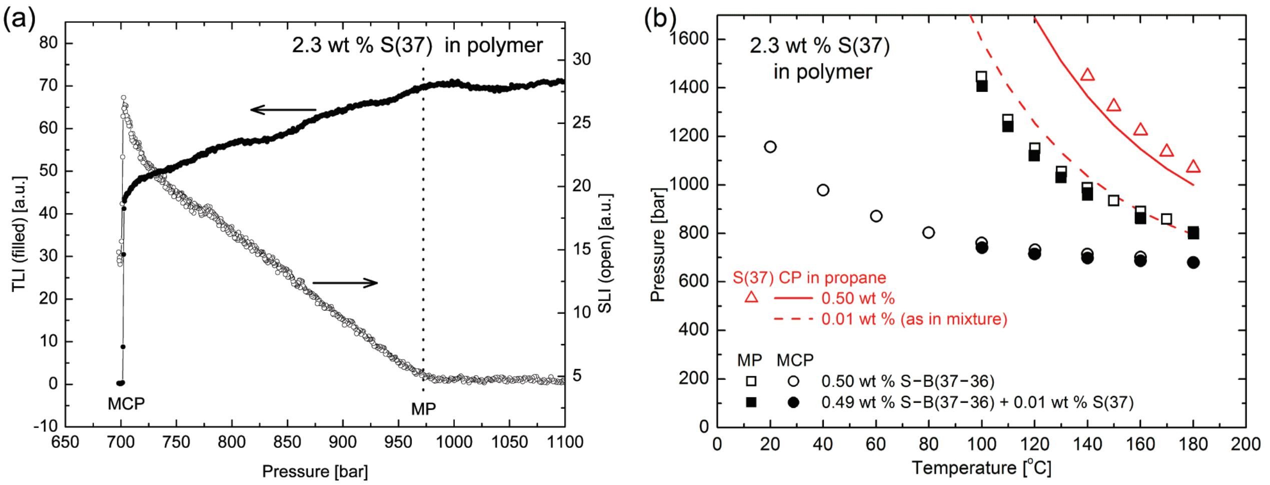

Figure 6. Micellization pressure (MP) and micellar cloud pressure (MCP) of polystyrene-*block*-polybutadiene, S−B(37−36), solution in propane with 2.3 wt % S(37): (a) transmitted- and scattered-light intensity trace at 140 °C; (b) pressure−temperature phase diagram with curves estimated by SAFT1.

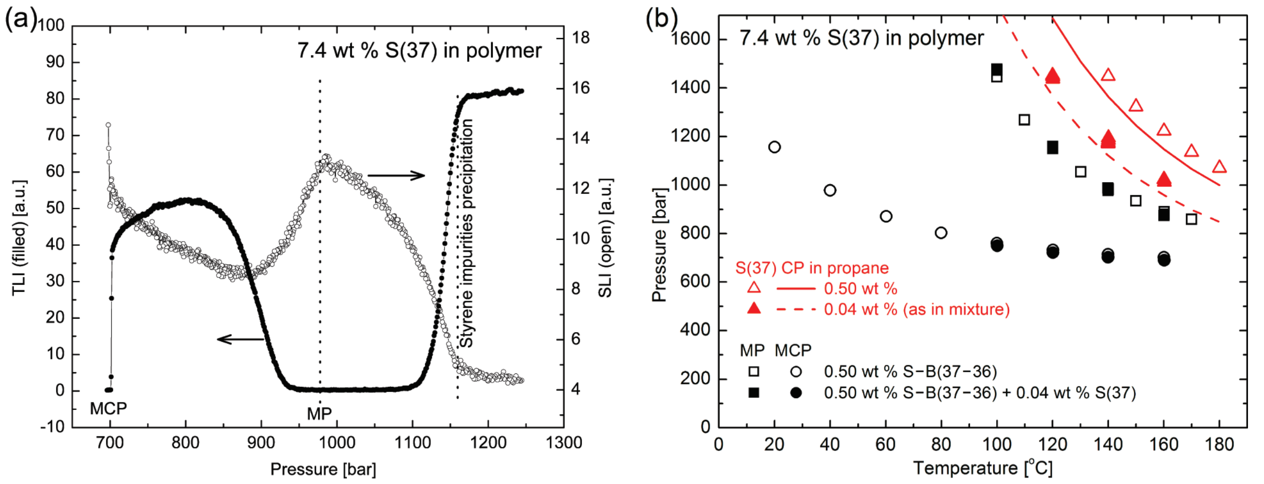

Figure 7. Micellization pressure (MP) and micellar cloud pressure (MCP) of polystyrene-*block*-polybutadiene, S−B(37−36), solution in propane with 7.4 wt % free polystyrene S(37): (a) transmitted- and scattered-light intensity trace at 140 °C; (b) pressure−temperature phase diagram with curves estimated by SAFT1.

matches the overall polymer concentration of the ternary solution (shown with filled circles and squares in Figure 6b). Perhaps more fitting, Figure 6b shows SAFT1-estimated CP (dashed curve) for a hypothetical 0.01 wt % polystyrene solution, which matches the S(37) concentration in the ternary solution. Significantly, the S(37) dashed curve is very close to the copolymer MP curve, which confirms two conjectures. First, block copolymer micellization must be driven by the precipitation of the core-forming block (polystyrene in this case), which is the essence of the pseudophase approximation.[9] Second, if free core-philic homopolymer (same as the core-forming block) is present in solution with the micelle-forming block copolymer, such a homopolymer is likely to be encapsulated in the micelle core. We do not have enough evidence at this point to prove it, or to suggest an exact mechanism of such an encapsulation upon decompression, but suspect that the copolymer micellization-induced encapsulation probably precedes the onset of bulk homopolymer precipitation or even significant density fluctuations in this case, rather than the other way around. Both of them, micellization/encapsulation and bulk separation, share the same thermodynamic driving force, that is, the polystyrene chemical potential that pushes its separation from propane, either in micelle cores or in a bulk phase. Now, let us consider consequences of increasing the polystyrene concentration in otherwise the same ternary solution.

The TLI and SLI traces for a solution richer in polystyrene, namely a 7.4 wt % S(37)-containing S−B(37−36) solution in propane, are shown in Figure 7a. This time, polystyrene is expected to start precipitating at slightly higher pressures, due to its higher concentration, clearly above the copolymer MP, as indicated by the sharp TLI drop to the lowest TLI around 1150 bar. On the other hand, SLI increases simultaneously with the TLI drop, which now can be due to S(37) precipitation, rather than micelle formation. However, in contrast to the SLI trace shown in Figure 6a, which increases upon decompression, this time further decompression causes SLI to drop, which leads to a characteristic "scattering" peak. The SLI drop can be explained by encapsulation of S(37) scatterers by the

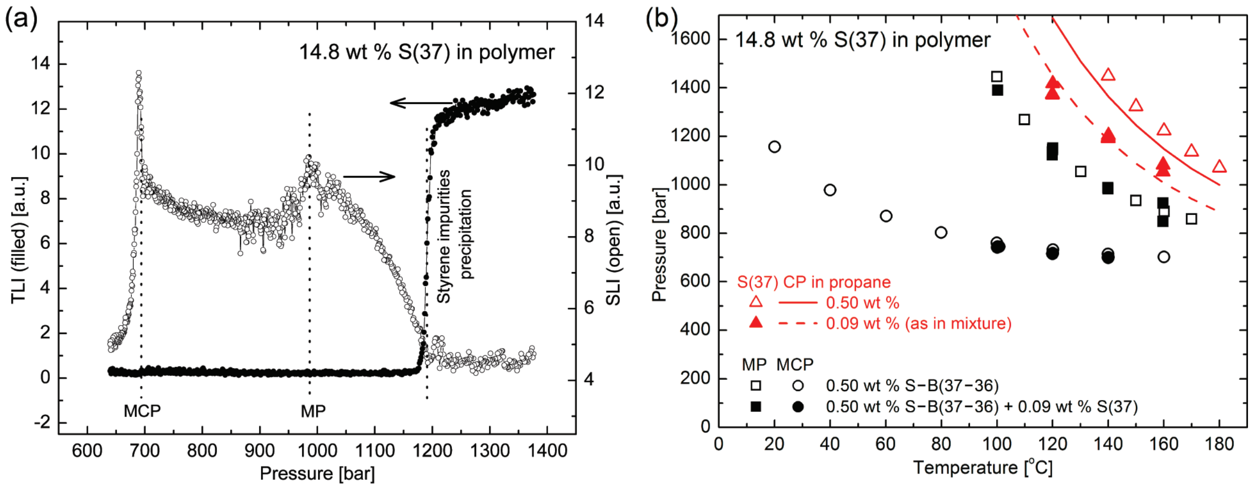

Figure 8. Micellization pressure (MP) and micellar cloud pressure (MCP) of polystyrene polystyrene-*block*-polybutadiene, S−B(37−36), solution in propane with 14.8 wt % S(37): (a) transmitted- and scattered-light intensity trace at 140 °C; (b) pressure−temperature phase diagram with curves estimated by SAFT1.

micelle cores. Since the onset of SLI increase is likely due to S(37) precipitation, as suggested by the sharp TLI drop, rather than due to micelle formation, it is safer instead to declare the SLI peak as a more accurate approximation of micellization pressure (MP). As more micelles are formed upon further decompression, TLI starts increasing at about 940 bar, and eventually SLI starts increasing as well. At an MCP of about 700 bar, a bulk phase separation occurs, as indicated by the sharp drop of TLI (and a less distinct drop of SLI due to bulk coalescence).

Figure 7b illustrates that, despite a 7.4 wt % S(37) content, the MCP and MP curves are still close to those for the plain S−B(37−36) solution. A binary 0.04 wt % polystyrene solution (matching the S(37) concentration in the ternary solution) phase separates at pressures and temperatures shown with a CP curve (dashed) predicted by SAFT1 in Figure 7b, which is roughly consistent with the filled triangles taken at the onset of the first TLI drop, around 1185 bar in Figure 7a. In other words, the SAFT1-calculated evidence for a copolymer-free solution, consistent with the experimental TLI evidence for a copolymer-containing solution, suggests that the onset of S(37) precipitation is close to but may slightly precede its encapsulation in copolymer micelles this time.

Despite the very different SLI and TLI traces, due to a higher polystyrene content, by a factor of 3 or so, the micellization pressures (MP) for the solutions shown in Figures 6 and 7 are almost the same. This suggests that MP, at the onset of micelle formation, is not perturbed by S(37), at least up to this concentration, despite the slight difference in MP detection methods (SLI drop in Figure 7 versus the onset of SLI increase in Figure 6). This is because S(37) in this case simply "precipitated" directly within the micelle cores, which means that 0.01 wt % is below the S(37) concentration threshold for the scattering peak associated with its bulk precipitation. On the other hand, S(37) in Figure 7 probably goes through the onset of bulk separation (cloud point) first, but at least a fraction of it is incorporated into the micelle cores as they are formed, which results in the scattering peak. At this point, it is not clear what fraction of polystyrene remains as a precipitated solid, if any, however unlikely, and what fraction is encapsulated. However it goes, the concentration threshold for the polystyrene encapsulation peak should be between 0.01 and 0.04 wt % (solution basis).

The TLI and SLI traces for a solution that is even richer in S(37), namely a 14.8 wt % S(37)-containing S−B(37−36) solution in propane, are shown in Figure 8a. As expected, the TLI drops sharply, and in contrast to Figure 7a, it does not recover upon decompression because, this time, there is enough precipitated free polystyrene to mask the encapsulation effect on TLI. Fortunately, while SLI initially increases upon S(37) precipitation, it drops upon its encapsulation by micelle cores, which leads to a scattering peak that is distinct enough to detect the micellization pressure (MP). The fact that TLI shown in Figure 8a does not recover upon encapsulation suggests that, for the system shown in Figure 8, the S(37) concentration probably exceeds the micelle encapsulation capacity (and hence a significant fraction of it remains in the form of precipitated solid). The encapsulation capacity is therefore estimated to be between 7.4 and 14.8 wt % on a solvent-free basis (or 0.04 and 0.09 wt % on an entire solution basis).

This example illustrates that SLI can uniquely detect micellization up to at least 15 wt % polystyrene, but much higher concentrations may prevent detection at some point. Again, we do not attempt to quantify how free polystyrene is distributed among the solution (probably very low fraction, if any), polystyrene-rich bulk phase, and micellar phase (micelle cores). Also, when we refer to polystyrene "precipitation" or "bulk separation", it is only in the context of observable changes in TLI and SLI, without suggesting any particular structure or stage of density fluctuation associated with an onset of such a bulk phase separation.

Figure 8b illustrates that, for a matching binary solution of 0.09 wt % S(37) alone in propane, the CP curve (dashed curve estimated from SAFT1 and consistent with the experimental points shown as filled triangles) is shifted up to somewhat higher pressures and temperatures relative to those shown in Figure 7b, which is due to the higher polystyrene concentration. However, as before, neither MCP, shown with circles, nor MP, shown with squares, is affected much by the presence of free polystyrene, at least up to this concentration. Now, what if one exchanges the S(37) solute that can be present in lower concentration but

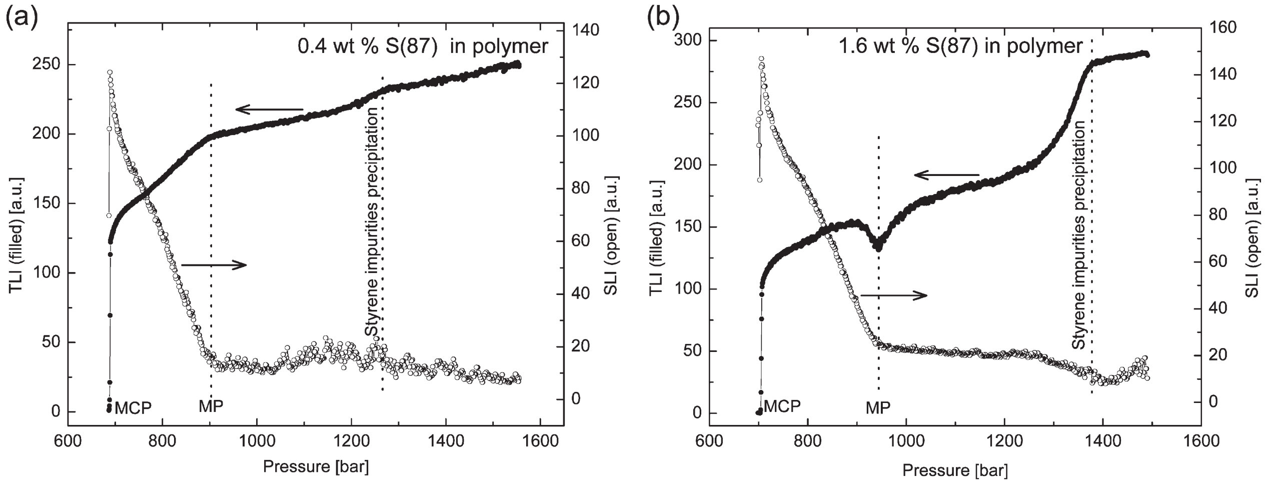

Figure 9. Transmitted- and scattered-light intensity trace for micellization pressure (MP) and micellar cloud pressure (MCP) of polystyrene-*block*-polybutadiene solution in propane with free polystyrene S(87) content of (a) 0.4 wt % and (b) 1.6 wt %, each at 150 °C.

matches the styrene block in size, by a much larger polystyrene solute, for example S(87) that matches or exceeds the size of the entire block copolymer?

Ternary Solutions: Polystyrene-*block*-polybutadiene and Copolymer-Sized Polystyrene in Propane. The TLI and SLI traces for such ternary solutions, namely for 0.4 wt % S(87)-containing and 1.6 wt % S(87)-containing S−B(37−36) solutions in propane, are shown in Figure 9. A slight to moderate TLI response is observed upon S(87) precipitation in both solutions, but the SLI response becomes somewhat noticeable only for the 1.6 wt % S(87) solution. Similar to what is observed for the plain copolymer solution shown in Figure 5 and for the 2.3 wt % solution shown in Figure 6, SLI for 0.4 wt % S(87) solution starts increasing and TLI starts decreasing, or decreasing more, at the MP, and they both drop sharply at MCP. The SLI response for the 1.6 wt % S(87) solution shown in Figure 9b is also similar; that is, SLI increases very slightly upon polystyrene precipitation and more so at the MP intercept. On the other hand, TLI initially recovers from its lowest value (local minimum) at around 930 bar indicated by the dotted line and then drops sharply at MCP. This is somewhat reminiscent of the 7.4 wt % S(37) solution behavior shown in Figure 7a, but this time TLI forms a negative peak at MP due to a lower polystyrene concentration, which makes it an alternative MP probe. The TLI increase for the 1.6 wt % S(87) solution shown in Figure 9b can be explained by encapsulation of S(87) molecules within the micelle core. In general, as expected, the larger polystyrene, S(87), precipitation and encapsulation are reflected in TLI and SLI traces and hence become detectable at lower concentrations than those for the smaller solute, S(37), but we do not attempt to pinpoint the exact precipitation and encapsulations limits and their molecular weight and concentration dependence in this work.

As for the other ternary solutions, MP and MCP for the ternary S(87) solutions are still within experimental reproducibility of those determined for the plain S−B(37−36) solution. This is shown in Figure 10 for the ternary solution that contains 0.4 wt % S(87) on a solvent-free basis (0.002 wt % solution basis), along with the calculated (curves) and experimental (triangles) CP data for the two corresponding binary solutions, one that matches the S(87) concentration in the ternary solution (0.002 wt %), and one that matches the overall polymer concentration (0.5 wt %). As before, the S(87) CP estimated from SAFT1 (curves) is consistent with the experimental data. The shift from the dashed curve to the solid curve illustrates the S(87) concentration effect on CP, in going from 0.002 to 0.5 wt %.

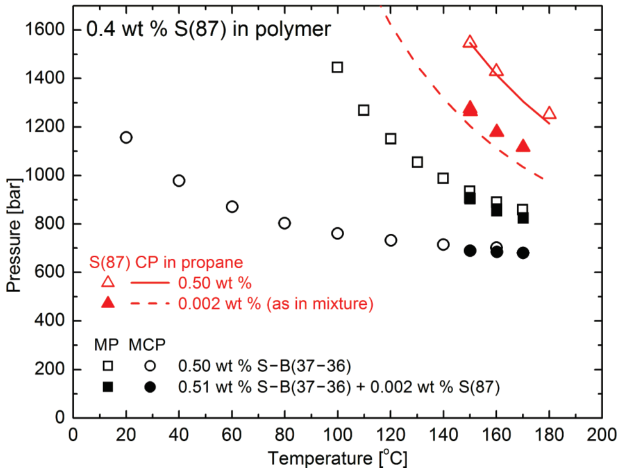

Figure 10. Micellization pressure (MP) and micellar cloud pressure (MCP) of polystyrene-*block*-polybutadiene solution in propane with 0.4 wt % free polystyrene S(87). The curves are estimated by SAFT1.

Such examples for uniform well-defined solutes, a micellizable diblock and a core-philic molecule, suggest general ideas of precipitation, micellization, encapsulation, and their detectability with transmitted- and scattered-light intensity upon decompression. For example, up to a certain concentration, say at least 15 wt % of S(37), the core-philic solute does not measurably alter the micellization pressure (MP) and micellar cloud pressure (MCP). While such a solute may complicate TLI and SLI analysis, in some instances, it may help detect the micelle formation. Figure 11 illustrates typical TLI and SLI responses in (a) a plain diblock copolymer solution and (b) a diblock copolymer mixed with a core-philic solute, such as polystyrene in this work, when its concentration range is just right, which needs to be calibrated for each system. In the example shown in Figure 11, which is realistic for the systems studied in this work, MP can be found

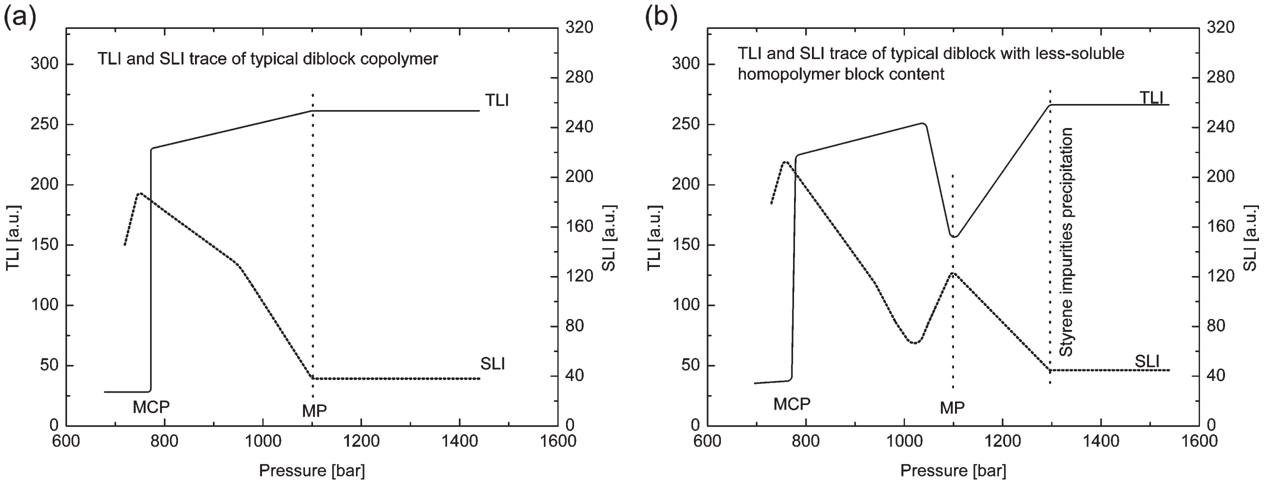

Figure 11. Typical transmitted- and scattered-light intensity trace of (a) pure diblock copolymer solution and (b) diblock copolymer solution with very low content of free less-soluble homopolymer.

around 1100 bar and the MCP around 780 bar for both solutions. The negative TLI peak upon micelle formation in Figure 11b depends on the concentration of the impurity. The corresponding SLI peak is the same as that usually referred to as the "anomalous micellization" observed for block copolymers in liquid solvents.[2,3] Analyzing such useful SLI and TLI traces helps understand the interplay of precipitation, micellization, and encapsulation and how they can be affected by the system properties.

Finally, for the record, while detailed characterization of the micelle size and shape is beyond the scope of this work, assuming spherical micelles, the hydrodynamic micelle diameters are found to increase as the polystyrene concentration increases, for example, from 73 nm for plain S−B(37−36) solution to 81 nm for a 7.4 wt % S(37)-containing S−B(37−36) solution in propane, at both 900 bar and 100 °C. More data, but no attempts at detailed analysis, are reported in the Supporting Information.

CONCLUSION

Pressure-tuned propane capacity and selectivity for polystyrene-*block*-polybutadiene can lead to random molecular solutions at high pressures, micellar solutions at moderate pressures, and bulk-separated micelles at low pressures. While corona-philic homopolymer solutes, such as polybutadiene, primarily stay in solution when the micelles are formed, a core-philic homopolymer solute, such as polystyrene, is found to concentrate in and hence become encapsulated by the micelle core. If the concentration of such a core-philic polystyrene solute is in the right range, say up to 15 wt % of a block-sized homopolymer on a solvent-free basis, it can produce an encapsulation peak on either the transmitted-light intensity trace or the scattered-light intensity trace, or both. Such encapsulation peaks can aid the micellization and encapsulation characterization, especially when guided by a reliable macromolecular model, such as statistical associating fluid theory (SAFT1), used to estimate the onset of bulk phase transitions in this work. A core-philic solute, free polystyrene in this case, can increase the micelle size upon encapsulation a bit, but it does not alter the crucial micellization pressure or even the micellar cloud pressure, at which the micelles coalesce and precipitate from solution in bulk.

ASSOCIATED CONTENT

Ⓢ Supporting Information. Tables of data. This material is available free of charge via the Internet at http://pubs.acs.org.

AUTHOR INFORMATION

Corresponding Author

*E-mail: radosz@uwyo.edu.

ACKNOWLEDGMENT

This work is funded by a National Science Foundation (Grants CTS-0625338, CBET-0828472, and CBET-1034530). Some of the copolymer samples were synthesized and characterized by Dr. Kunlun Hong in Prof. Jimmy Mays' group at Oak Ridge National Laboratory's Center for Nanophase Materials Sciences, through User Project CNMS2006-114, sponsored by the Scientific User Facilities Division, Office of Basic Energy Sciences, U.S. Department of Energy. The authors are grateful to the anonymous journal Reviewer 3 whose penetrating, thoughtful, and illuminating comments helped improve this manuscript.

REFERENCES

(1) Vaidya, N. Y.; Han, C. D. *Polymer* **2002**, *43*, 3047–3059.

(2) Zhou, Z.; Chu, B. *Macromolecules* **1988**, *21*, 2548–2554.

(3) Lodge, T. P.; Bang, J.; Hanley, K. J.; Krocak, J.; Dahlquist, S.; Sujan, B.; Ott, J. *Langmuir* **2003**, *19*, 2103–2109.

(4) Winoto, W.; Adidharma, H.; Shen, Y.; Radosz, M. *Macromolecules* **2006**, *39*, 8140–8144.

(5) Winoto, W.; Tan, S. P.; Shen, Y.; Radosz, M.; Hong, K.; Mays, J. W. *Macromolecules* **2009**, *42*, 3823–3826.

(6) Winoto, W.; Tan, S. P.; Shen, Y.; Radosz, M.; Hong, K.; Mays, J. W. *Macromolecules* **2009**, *42*, 7155–7163.

(7) Winoto, W.; Radosz, M.; Hong, K.; Mays, J. W. *J. Non-Cryst. Solids* **2009**, *355*, 1393–1399.

(8) Winoto, W.; Shen, Y.; Radosz, M.; Hong, K.; Mays, J. W. *J. Phys. Chem. B* **2009**, *113*, 15156–15161.

(9) Tan, S. P.; Winoto, W.; Radosz, M. *J. Phys. Chem. C* **2007**, *111*, 15752–15758.

(10) Hadjichristidis, N.; Pitsikalis, M.; Pispas, S.; Iatrou, H. *Chem. Rev.* **2001**, *101*, 3747–3792.

(11) Uhrig, D.; Mays, J. W. *J. Polym. Sci., Part A: Polym. Chem.* **2005**, *43*, 6179–6222.

(12) Hattam, P.; Gauntlett, S.; Mays, J. W.; Hadjichristidis, N.; Young, R. N.; Fetters, L. J. *Macromolecules* **1991**, *24*, 6199–6209.

(13) Mays, J.; Hadjichristidis, N.; Fetters, L. J. *Macromolecules* **1984**, *17*, 2723–2728.

(14) Tan, S. P.; Meng, D.; Plancher, H.; Adidharma, H.; Radosz, M. *Fluid Phase Equilib.* **2004**, *226*, 189–194.

(15) Adidharma, H.; Radosz, M. *Ind. Eng. Chem. Res.* **1998**, *37*, 4453–4462.